AMERICAN SOCIETY FOR MICROBIOLOGY | Infection and Immunity

The First Histidine Triad Motif of PhtD Is Critical for Zinc Homeostasis in *Streptococcus pneumoniae*

Bart A. Eijkelkamp, Victoria G. Pederick, Charles D. Plumptre, Richard M. Harvey, Catherine E. Hughes, James C. Paton, Christopher A. McDevitt

Research Centre for Infectious Diseases, School of Biological Sciences, University of Adelaide, Adelaide, Australia

***Streptococcus pneumoniae* is the world's foremost human pathogen. Acquisition of the first row transition metal ion zinc is essential for pneumococcal colonization and disease. Zinc is acquired via the ATP-binding cassette transporter AdcCB and two zinc-binding proteins, AdcA and AdcAII. We have previously shown that AdcAII is reliant upon the polyhistidine triad (Pht) proteins to aid in zinc recruitment. Pht proteins generally contain five histidine (His) triad motifs that are believed to facilitate zinc binding and therefore play a significant role in pneumococcal metal ion homeostasis. However, the importance and potential redundancy of these motifs have not been addressed. We examined the effects of mutating each of the five His triad motifs of PhtD. The combination of *in vitro* growth assays, active zinc uptake, and PhtD expression studies show that the His triad closest to the protein's amino terminus is the most important for zinc acquisition. Intriguingly, *in vivo* competitive infection studies investigating the amino- and carboxyl-terminal His triad mutants indicate that the motifs have similar importance in colonization. Collectively, our new insights into the contributions of the individual His triad motifs of PhtD, and by extension the other Pht proteins, highlight the crucial role of the first His triad site in zinc acquisition. This study also suggests that the Pht proteins likely play a role beyond zinc acquisition in pneumococcal virulence.**

Streptococcus pneumoniae is responsible for a broad range of major human diseases, including pneumonia, sepsis, meningitis, and otitis media, which together contribute to significant global morbidity and mortality (1). The ability of the bacterium to import zinc (Zn^{2+}) ions from the extracellular environment is critical for its pathogenicity (2–5). Pneumococcal Zn^{2+} acquisition occurs via the cluster A-I substrate binding proteins (SBPs), AdcA and AdcAII, which deliver the metal ion to AdcCB, the ATP-binding cassette transporter, for cellular import (2–4).

The polyhistidine triad (Pht) family of proteins have also been shown to contribute to pneumococcal Zn^{2+} acquisition (4–6). *S. pneumoniae* encodes four related Pht proteins, PhtA, PhtB, PhtD, and PhtE, which are thought to be predominantly anchored in the pneumococcal cell wall (7, 8). The exposure of the Pht proteins on the cell surface has led to significant investigation into their potential use in next-generation pneumococcal vaccines, with clinical trials up to phase II having been completed (9–13). Despite this, their contribution to Zn^{2+} acquisition has only recently been revealed. A role for the Pht proteins in scavenging transition metal ions was initially reported by Rioux et al. (14), and it was subsequently suggested that PhtD and AdcAII could interact to transfer Zn^{2+} from the former to the latter (8, 15). Recently, we showed that AdcAII is largely dependent on the Pht proteins to acquire Zn^{2+} under Zn^{2+}-limiting conditions. In contrast, AdcA is capable of contributing to Zn^{2+} acquisition independent of the Pht proteins, likely via its histidine-rich loop and C-terminal ZinT domain, features that are absent from AdcAII (4). Consistent with the high level of similarity between PhtA, PhtB, PhtD, and PhtE, each of the four Pht proteins has been shown to contribute to AdcAII-mediated Zn^{2+} acquisition (5). Furthermore, deletion of the *pht* genes in an Δ*adcAII* mutant reduced pneumococcal invasion relative to the parental Δ*adcAII* strain, indicating that the Pht proteins hold roles in addition to AdcAII-mediated Zn^{2+} acquisition (5). Currently, it is not known whether these other functions are related to zinc homeostasis.

The defining feature of the Pht proteins is the presence of multiple copies of the histidine triad motif (HxxHxH). PhtD, the most highly conserved Pht protein across pneumococcal strains, contains five His triad (HT) motifs, and each motif is thought to bind one Zn^{2+} ion (8). Loisel et al. produced a truncated derivative of PhtD containing only one HT motif and determined the affinity of the fragment for Zn^{2+} to be 131 ± 10 nM, which is weaker than that of AdcA (2.4 ± 0.1 nM) and other Zn^{2+}-binding cluster A-I SBPs (4, 8, 16). This is consistent with the model for Zn^{2+} transfer to the higher-affinity site of a Zn^{2+}-binding SBP for transport into the bacterial cell. The structure of this PhtD fragment has also been analyzed by nuclear magnetic resonance spectroscopy, with the single His triad site shown to bind Zn^{2+} in an assumed tetrahedral conformation by His83 (Nε2), His86 (Nε2), His88 (Nδ1), and Glu63 (15). This structure shows similarities to that previously derived by X-ray crystallography for a truncated PhtA fragment, which contained a different HT motif (17). In both cases, the motifs were observed to comprise part of a three-stranded β-sheet, and this suggests that a similar secondary structure could occur in the full-length Pht proteins (15, 17). However, it is important to note that these observations were made from truncated Pht fragments; their relevance to the full-length proteins remains

Received 21 August 2015 **Returned for modification** 25 October 2015
Accepted 8 November 2015

Accepted manuscript posted online 16 November 2015

Citation Eijkelkamp BA, Pederick VG, Plumptre CD, Harvey RM, Hughes CE, Paton JC, McDevitt CA. 2016. The first histidine triad motif of PhtD is critical for zinc homeostasis in *Streptococcus pneumoniae*. Infect Immun 84:407–415. doi:10.1128/IAI.01082-15.

Editor: A. Camilli

Address correspondence to Christopher A. McDevitt, christopher.mcdevitt@adelaide.edu.au.

TABLE 1 Strains used in this study

S. pneumoniae strain	Description or characteristic(s)	Source or reference
D39	Serotype 2 parent strain	NCTC7466
Δ*adcA* mutant	D39 with *adcA* deleted	4
Δ*adcA* Δ*phtABE* mutant	*adcA*, *phtA*, *phtB*, and *phtE* deleted	5
HT1	Δ*adcA* Δ*phtABE* mutant with HT site 1 mutated	This study
HT2	Δ*adcA* Δ*phtABE* mutant with HT site 2 mutated	This study
HT3	Δ*adcA* Δ*phtABE* mutant with HT site 3 mutated	This study
HT4	Δ*adcA* Δ*phtABE* mutant with HT site 4 mutated	This study
HT5	Δ*adcA* Δ*phtABE* mutant with HT site 5 mutated	This study
Δ*adcA* Δ*phtABDE* mutant	*adcA*, *phtA*, *phtB*, *phtD*, and *phtE* deleted	5

to be confirmed. Further, there is a paucity of information on the flexibility and movement of SBPs and whether they could colocalize with the Pht proteins to effect Zn^{2+} transfer.

To date, there has been no investigation into the role of the HT motifs in the context of intact pneumococci or on their potential contribution to the process of Zn^{2+} uptake or to the other proposed functions of the proteins. Since these motifs are the defining feature of this protein family, with each of the Pht proteins sharing significant sequence similarity and contributing to Zn^{2+} acquisition, we have addressed these questions by examining the phenotypes of five PhtD mutant strains, each lacking one of the five HT motifs.

MATERIALS AND METHODS

Strains and growth media. Defined, nonpolar deletion replacement or unmarked deletion mutants of *phtA*, *phtB*, *phtD*, *phtE*, or *adcA* in *S. pneumoniae* D39 have been generated previously (4, 18) (Table 1). To modify the HT motifs of PhtD, forward and reverse primers were designed complementary to the sequences encoding the motifs and were paired with primers flanking *phtD* to perform PCR to amplify the gene in two parts. The primers were designed with mutations to substitute phenylalanine residues in place of each histidine residue of the relevant triad (Table 2). The two PCR products were then fused by overlap extension PCR and used to transform the Δ*adcA* Δ*phtABE* strain, resulting in the mutant strains designated HT1 to HT5, respectively. Each of these strains produced a mutant variant of PhtD wherein each of the His residues of one of the five HT motifs had been substituted by phenylalanine residues. Mutagenesis of *phtD* in the HT strains was confirmed by DNA sequencing. Opaque phase variants were used in all experiments and a complete list of strains used in this study is in Table 1. Bacteria were routinely grown at 37°C in 5% CO_2 on Columbia agar supplemented with 5% (vol/vol) horse blood or, for challenge of mice, in serum broth (10% heat-inactivated horse serum in nutrient broth). Alternatively, cation-defined medium (CDM; prepared as described previously [4, 19, 20]) was used. To assess the effect of Zn^{2+} starvation, the Zn(II)-chelating agent *N*,*N*,*N*′,*N*′-tetrakis(2-pyridylmethyl)ethylenediamine (TPEN) was supplemented at an equimolar concentration to Zn^{2+}, as determined in CDM by inductively coupled plasma-mass spectrometry (ICP-MS) to yield CDM-TPEN. To examine growth kinetics, cells were harvested from Columbia agar plates supplemented with 5% (vol/vol) horse blood incubated for 18 h at 37°C in 5% CO_2 and inoculated in CDM(-TPEN) to an optical density at 600 nm (OD_{600}) of 0.01. For all other analyses, cells were harvested similarly, but CDM-TPEN cultures were inoculated at an OD_{600} of 0.05.

Growth analysis. For growth analyses, *S. pneumoniae* D39 and mutant strains were grown in CDM with 1 μM $MnSO_4$ until they reached an OD_{600} of 0.3. They were then subcultured into 200 μl CDM or CDM-TPEN to a final OD_{600} of 0.01. The bacteria were incubated at 37°C in a CO_2-enriched atmosphere, and growth was monitored by measurement of the OD_{600} at 30-min intervals.

Flow cytometry. Flow cytometry was performed essentially as described previously (11). In brief, cells were grown in CDM-TPEN until they reached an OD_{600} of 0.3 and incubated for 1 h at 37°C with murine anti-PhtD antisera in phosphate-buffered saline (PBS) (1:100 [vol/vol]) generated previously (11), followed by Alexa Fluor 488-rabbit anti-mouse IgG(H+L) (Thermo Fisher Scientific) for 30 min at 4°C. The cells were washed three times in 1 ml of PBS between each step. Fluorescence measurements from 10,000 events were collected using a BD FACSCanto flow cytometer (BD Biosciences). Data were analyzed by using the software

TABLE 2 Oligonucleotides used in this study

Primer[a]	Sequence (5′−3′)[b]
16s_F (qRT-PCR)	CATGCAAGTAGAACGCTGAA
16s_R (qRT-PCR)	TGTCATGCAACATCCACTCT
phtD_F (qRT-PCR)	GTATTAGACAAAATGCTGTGGAG
phtD_R (qRT-PCR)	CTGTATAGGAGTCGGTTGACTTTC
HT1_F	ATGTGACCTCT**TTT**GGAGAC**TTC**TAT**TTT**TACTATAATGGCAAGGTTC
HT1_R	GAACCTTGCCATTATAGTA**AAA**ATA**GAA**GTCTCC**AAA**AGAGGTCACAT
HT2_F	ATCGTTCCT**TTC**GGCGAC**TTT**TAC**TTT**TACATTCCTAAGAGTGATTTG
HT2_R	CAAATCACTCTTAGGAATGTA**AAA**GTA**AAA**GTCCCC**GAA**AGGAACGAT
HT3_F	GCTGTACCG**TTC**GGAGAC**TTT**TAT**TTT**TTTATTCCTTATTCACAACTG
HT3_R	CAGTTGTGAATAAGGAATAAA**AAA**ATA**AAA**GTCTCC**GAA**CGGTACAGC
HT4_F	CCTATGTAACTCCA**TTT**ATGACC**TTT**AGC**TTC**TGGATTAAAAAAGATAG
HT4_R	CTATCTTTTTTAATCCA**GAA**GCT**AAA**GGTCAT**AAA**TGGAGTTACATAGG
HT5_F	AGTTTAATCATACCT**TTT**TATGAC**TTT**TAC**TTT**AACATCAAATTTGAGT
HT5_R	ACTCAAATTTGATGTT**AAA**GTA**AAA**GTCATA**AAA**AGGTATGATTAAACT

[a] The direction of the primer is indicated by the primer designation suffix (F, forward; R, reverse).
[b] Nucleotides targeting histidine residues for mutation to phenylalanine are indicated in boldface.

package FlowJo (Tree Star). The results are a single representative of two independent experiments.

Whole-cell metal ion accumulation. *S. pneumoniae* strains were grown in CDM-TPEN to an OD_{600} of 0.3, and their metal ion content was determined essentially as described previously (21). In brief, the bacteria were washed three times with PBS containing 5 mM EDTA and then twice with PBS. Bacterial pellets were desiccated by heating at 95°C overnight. The dry cell weight was measured, and the pellets were resuspended in 35% HNO_3. Metal ion content was measured on an Agilent 7500cx inductively coupled plasma-mass spectrometer.

Measuring intracellular zinc using FluoZin-3. *S. pneumoniae* strains were grown in CDM to an OD_{600} of 0.3. The cells were then washed three times in PBS, incubated with 5 μM cell permeant FluoZin-3 AM, probenecid, and PowerLoad (Thermo Fisher Scientific), and further mixed for 30 min at room temperature, similar to a method described previously (22). After washing in PBS to remove extracellular FluoZin-3 AM, the fluorescence was measured (excitation, 494 nm; emission, 516 nm). $ZnSO_4$ was added to a final concentration of 10 μM, and the fluorescence was examined after 20 min. The data, corrected to cells not supplemented with $ZnSO_4$, represent the mean of at least three independent experiments. Statistical significance was assessed by one-way analysis of variance (ANOVA) using Dunnett's posttest, comparing each strain to the Δ*adcA* Δ*phtABE* strain.

Quantitative immunoblot and qRT-PCR analyses. Wild-type and mutant *S. pneumoniae* strains were grown under the same conditions as for ICP-MS. After reaching an OD_{600} of 0.3, samples were taken for protein analysis and RNA extraction. For protein extraction, cells were incubated with 0.1% sodium deoxycholate (Sigma-Aldrich) at 37°C for 60 min to induce lysis. Protein concentrations were determined (DC Bio-Rad protein assay; Bio-Rad), and 20 μg of total protein was loaded into each lane of a 4 to 12% NuPage Bis-Tris gel. After electrophoretic separation by SDS-PAGE, the proteins were transferred to a nitrocellulose membrane using an iBlot system (Thermo Fisher Scientific). Blots were incubated with previously generated murine antisera against PhtD (11). This was followed by incubation with anti-mouse IRDye 800 and analysis using an Odyssey infrared imaging system (LI-COR). Band intensities were measured using the manufacturer's application software. The results are representative of three independent experiments. For RNA extraction and quantitative reverse transcription-PCR (qRT-PCR) analysis, 500 μl of culture was mixed with 1 ml of RNA protect (Qiagen). RNA was extracted and purified using an RNeasy Protect Bacteria minikit (Qiagen) after enzymatic lysis using lysozyme and mutanolysin, according to the manufacturer's instructions. The total RNA samples were treated with DNase I (Roche) and qRT-PCR was carried out using a SuperScript III One-Step RT-PCR kit (Thermo Fisher Scientific) on an LC480 real-time cycler (Roche). Transcription levels of genes analyzed were normalized to those obtained for 16S rRNA. Primer sequences are available in Table 2. The results were representative of three independent experiments.

Assessment of bacterial fitness. Outbred 5- to 6-week-old female CD1 (Swiss) mice were used in all animal experiments. Mice were anesthetized by intraperitoneal injection of pentobarbital sodium (Nembutal; Rhone-Merieux) at a dose of 66 μg per g of body weight, followed by intranasal administration of 50 μl of bacterial suspension containing $\sim 10^7$ CFU. For competition experiments, 5×10^6 CFU of each of the two relevant strains was mixed prior to intranasal administration. The challenge dose was confirmed retrospectively by serial dilution and plating on blood agar, and for competition experiments, this was followed by patching of colonies onto blood agar plates with or without antibiotic to allow discrimination of the two strains.

At 24 h (absolute counts) and 48 h (absolute counts and competition) postchallenge, mice were euthanized by CO_2 asphyxiation. Blood was collected by syringe from the posterior vena cava. The pleural cavity was lavaged with 1 ml of sterile PBS introduced through the diaphragm. Pulmonary vasculature was perfused by infusion of sterile PBS through the heart. Lungs were subsequently excised. The trachea was then exposed, and 1 ml of PBS was inserted into the tracheal end of the upper respiratory tract and collected from the nose (nasal wash). Lastly, the nasopharynx/upper palate was excised (nasal tissue). Tissues were homogenized, and all samples were serially diluted and plated on blood agar. For competition experiments, colonies were subsequently patched onto blood plates with or without the relevant antibiotic to allow discrimination of the two mutant strains and determination of output ratios. Competitive indices (the ratio of one mutant strain to the other relative to the input ratio) were then calculated and compared to a theoretical value of 1 (which would indicate no difference in fitness between strains) by one-sample *t* tests.

All procedures performed here were conducted with a view to minimizing the discomfort of the animals and used the minimum numbers to generate reproducible and statistically significant data. All experiments were approved by the University of Adelaide Animal Ethics Committee (Animal Welfare Assurance number A5491-01; project approval number S-2013-053) and were performed in strict adherence to guidelines dictated by the Australian Code of Practice for the Care and Use of Animals for Scientific Purposes.

RESULTS

Mutation of the HT sites results in compromised growth under Zn^{2+}-limiting conditions. Zinc recruitment under Zn^{2+}-replete conditions occurs via AdcA and AdcAII in the pneumococcus. AdcAII has a more significant role during Zn^{2+} deficiency due to its high level of upregulation under such conditions. However, AdcAII relies on the Pht proteins for full functionality. To examine the role of the HT motifs in the Pht proteins, mutants lacking one of the five HT motifs in PhtD were constructed in a previously generated Δ*adcA* Δ*phtABE* background strain. In these mutant strains, Zn^{2+} acquisition was entirely dependent upon AdcAII and the four remaining functional HT motifs of PhtD. In this way, the contribution of the individual HT sites could be examined. The PhtD HT motifs have been designated HT1 to HT5, with HT1 at the amino terminus predicted to be closest to the cell membrane and HT5 at the carboxyl terminus closest to the extracellular environment (14, 23, 24). In the HT mutants, each of the histidine residues (HxxHxH) have been mutated to phenylalanine, removing their Zn^{2+} binding capacity while maintaining a similar steric bulk. The HT mutant strains were assessed for growth *in vitro* in comparison to the wild-type strain D39, the Δ*adcA* Δ*phtABE* mutant strain (direct parent strain), and the Δ*adcA* Δ*phtABDE* mutant strain (lacking all Pht proteins). Growth of all mutant strains remained essentially unchanged compared to that of the wild type in CDM, i.e., Zn^{2+}-replete conditions (Fig. 1A). To examine the effect of Zn^{2+} limitation on growth of these strains, the medium was supplemented with the Zn^{2+}-chelating agent TPEN at an equimolar concentration to the Zn^{2+} present in the media. In general, these stress conditions affected growth of all strains, including the wild type, but to vastly different extents (Fig. 1B). Most strikingly, growth was largely inhibited in the HT1 mutant, a phenotype similar to that seen for the Δ*adcA* Δ*phtABDE* mutant, indicating that mutation of HT1 abolished the functionality of PhtD in Zn^{2+} recruitment. The HT2 and HT3 mutants also showed compromised growth, but not to the same extent as the HT1 mutant. In contrast, the HT4 and HT5 mutants had growth phenotypes that were essentially identical to that of the parental strain (Δ*adcA* Δ*phtABE*). Taken together, these results indicate a potential hierarchy in the HT sites for their importance in growth under Zn^{2+} limited conditions, with the relative contribution of each of the sites to Zn^{2+} ac-

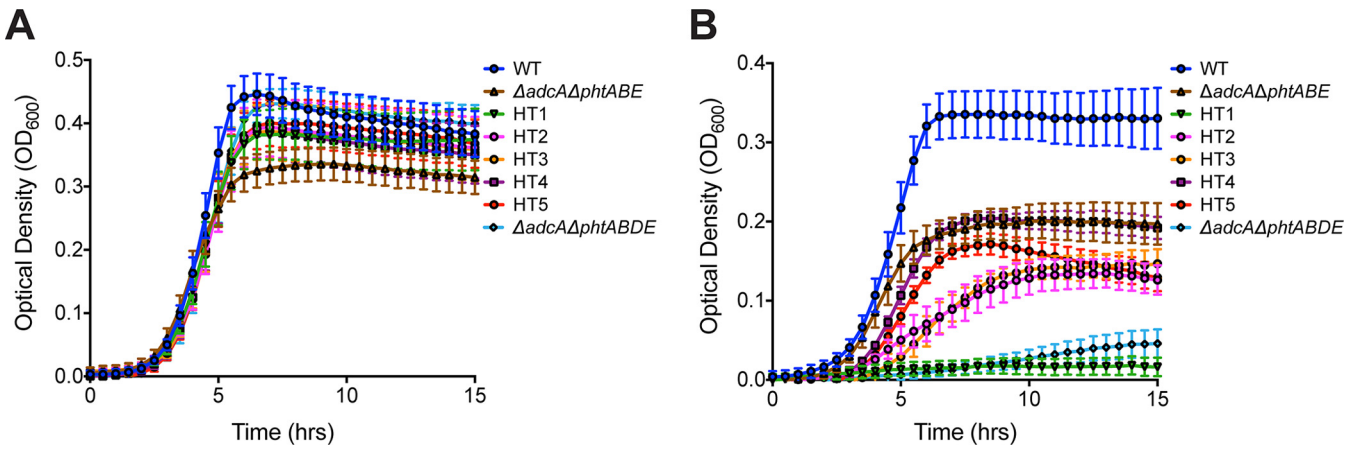

FIG 1 *In vitro* growth comparison of the *S. pneumoniae* HT mutant strains. Bacteria were grown in CDM (A) or CDM-TPEN (B) (i.e., under Zn^{2+}-restricted conditions) at 37°C, and growth was monitored by OD_{600} measurements every 30 min. Data are representative mean OD_{600} measurements ± the standard errors of the mean (SEM) from three independent biological experiments. WT, wild type.

quisition generally decreasing from the amino terminus to the carboxyl terminus of the protein (HT sites 1 to 5).

The HT mutants express PhtD at the cell surface. To ascertain whether the differences in the growth kinetics of the HT site mutants under Zn^{2+}-limiting conditions were due to expression issues and/or mislocalization of PhtD, we examined the strains for surface-localized PhtD by flow cytometry. Cells were incubated with an anti-PhtD antiserum, followed by a fluorescently labeled secondary antibody, to determine the presence of cell surface PhtD, as previously described (11). Consistent with expectations, the Pht-null mutant (Δ*adcA* Δ*phtABDE*) showed a single population representing negative events, similar to that seen for the unlabeled wild-type sample (Fig. 2). The labeled wild-type and Δ*adcA* strains showed a similar pattern to each other, with a broad distribution of fluorescence intensities seen, indicating that PhtD was expressed but to substantially different levels. The combined deletion of *adcA*, *phtA*, *phtB*, and *phtE* (Δ*adcA* Δ*phtABE*) resulted in a dramatic shift, with most cells showing ~10-fold-higher fluorescence levels than the Δ*adcA* strain. Subsequent mutation of the HT sites resulted in only minor changes compared to the parental strain, indicating that mutation of the HT sites did not have a detrimental impact on PhtD localization. However, the flow cytometric analyses of the HT1 mutant, and to some extent the HT2 mutant, indicate that PhtD may be expressed at even higher levels in these mutant strains than in the parent strain (Δ*adcA* Δ*phtABE*).

Mutation of PhtD HT1 results in increased PhtD expression. To gain greater insight into potential differences in the abundance of PhtD, as revealed by our flow cytometric analyses, we examined the transcript levels of *phtD*, which is part of the Zn^{2+}-responsive AdcR regulon (25). Deletion of *adcA* resulted in a minor increase in *phtD* transcription (~3-fold) and the additional deletion of *phtA*, *phtB*, and *phtE* (Δ*adcA* Δ*phtABE*) resulted in an ~4.4-fold increase in expression, compared to the wild type (Fig. 3A). Mutation of the PhtD HTs in the Δ*adcA* Δ*phtABE* strain revealed highly intriguing differences. Compared to the Δ*adcA* Δ*phtABE* parental strain, the HT1 mutant showed a significant 10-fold ($P < 0.0001$) upregulation of *phtD*. Despite a modest increase in *phtD* expression in the HT2, HT3, HT4, and HT5 mutants (2.5- to 3.1-fold), this was not significantly different from the Δ*adcA* Δ*phtABE* strain. Examination of PhtD protein expression by quantitative immunoblot analysis showed a pattern consistent with the mRNA levels. However, the overall extent of the differences between strains was more modest (Fig. 3B and C). Minor,

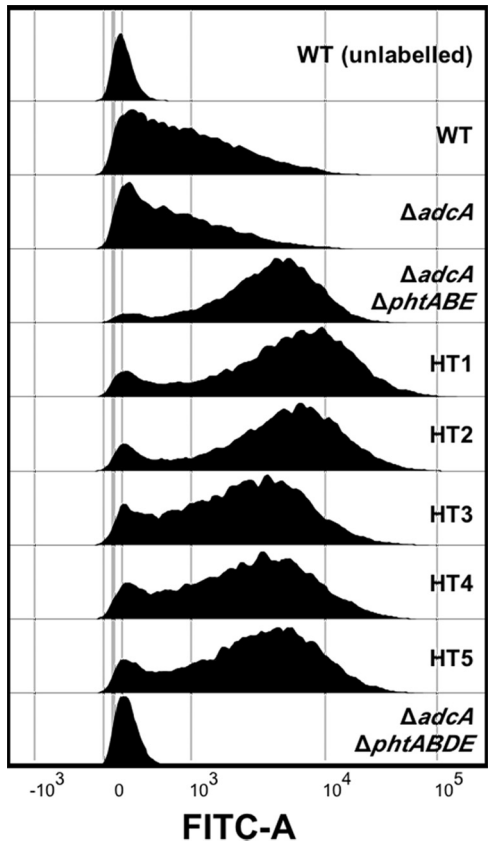

FIG 2 Flow cytometric measurement of the presence of PhtD at the bacterial surface of the HT mutants and control strains. A representative histogram of fluorescence profiles for each strain is shown. An unlabeled wild-type strain (WT) and a *phtD* deletion strain (Δ*adcA* Δ*phtABDE*) were included to represent the profiles of negative cells.

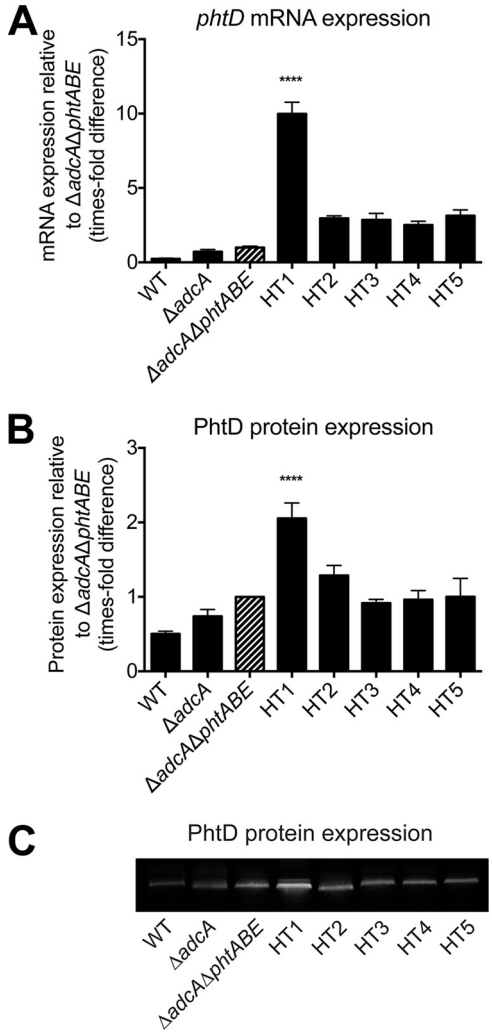

FIG 3 Analysis of PhtD expression levels in HT mutant strains grown in CDM-TPEN. mRNA (A) and protein (B) expression levels are shown, normalized to the levels in the Δ*adcA* Δ*phtABE* strain. For mRNA, measurements were made relative to 16S rRNA. Strains were compared to the Δ*adcA* Δ*phtABE* mutant (striped bars) by one-way ANOVA using Dunnett's posttest, and statistically significant differences, where present, are indicated (****, $P < 0.0001$). The results (± the SEM) are representative of three independent experiments. WT, wild type. (C) Representative Western blot for the determination of PhtD protein expression.

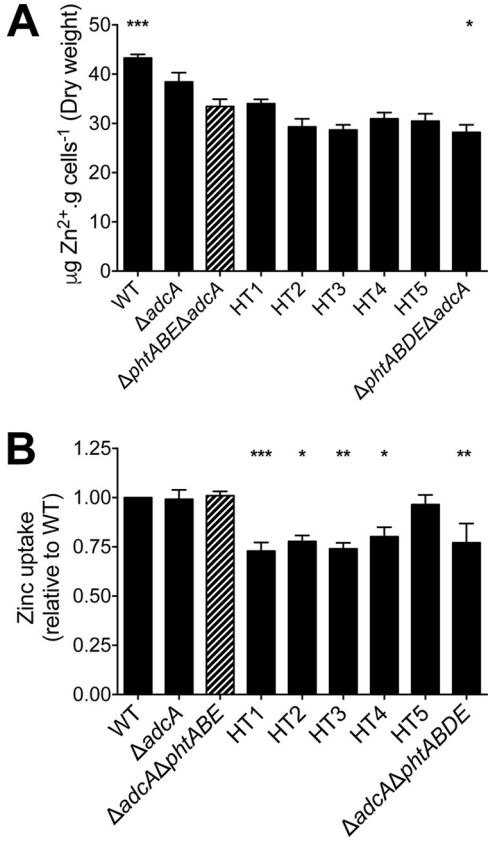

FIG 4 (A) Whole-cell Zn^{2+} accumulation of control and HT mutant strains as determined by ICP-MS. (B) FluoZin-3 AM Zn^{2+} uptake assay examining control and HT mutant strains. Zinc uptake for each of the strains is shown relative to that for the wild type. In both assays, all strains were compared to the Δ*adcA* Δ*phtABE* mutant (striped bars) by one-way ANOVA using Dunnett's posttest, and statistical significance is indicated (*, $P < 0.05$; **, $P < 0.01$; ***, $P < 0.001$). Data are means (± the SEM) from a minimum of three biological replicates.

nonsignificant differences in PhtD expression were observed for the Δ*adcA* and Δ*adcA* Δ*phtABE* strains compared to the wild type. However, the HT1 mutant displayed a significant 2-fold ($P < 0.0001$) increase in expression of PhtD relative to its Δ*adcA* Δ*phtABE* parent strain. In contrast, the HT2 mutant exhibited a statistically insignificant increase in PhtD expression (1.3-fold), with the expression of PhtD in the HT3, HT4 and HT5 mutants unchanged compared to that in the Δ*adcA* Δ*phtABE* strain. Taken together, since *phtD* is upregulated by the Zn^{2+}-dependent transcription regulator AdcR in response to Zn^{2+} deficiency, these data strongly suggest that mutation of HT site 1 resulted in a significantly lower level of Zn^{2+} within the pneumococcus.

Metal ion accumulation of HT deficient strains. To further examine the effect of mutating the HT motifs of PhtD, the cellular metal content of the HT mutant, wild-type, and control strains was assessed following growth in CDM-TPEN to an OD_{600} of 0.3. Consistent with our previous observations, deletion of *adcA* in conjunction with *phtA*, *phtB*, and *phtE* (Δ*adcA* Δ*phtABE*) resulted in a significant reduction in cellular Zn^{2+} abundance relative to that for the wild type ($P < 0.001$) as determined by ICP-MS (Fig. 4A) (5). Although only minor, the additional deletion of *phtD* (Δ*adcA* Δ*phtABDE*) resulted in a further reduction in Zn^{2+} accumulation (15%; $P < 0.05$). Due to the minimal difference in Zn^{2+} accumulation between the Δ*adcA* Δ*phtABE* and Δ*adcA* Δ*phtABDE* strains, the effect of mutating the individual HT sites on total cellular Zn^{2+} accumulation was not able to be resolved via ICP-MS. To ascertain whether the HT mutant strains had differences in the ability to acquire Zn^{2+}, we performed a Zn^{2+} uptake assay using the intracellular Zn^{2+}-responsive fluorophore FluoZin-3 AM. Analysis of the strains revealed similar levels of Zn^{2+} uptake in the wild-type, Δ*adcA*, and Δ*adcA* Δ*phtABE* strains after the addition of $ZnSO_4$ (Fig. 4B). Thus, the combined action of AdcAII and PhtD is sufficient for wild-type levels of Zn^{2+} uptake. In the absence of AdcA and all four Pht proteins, the Δ*adcA* Δ*phtABDE* strain exhibited a significant decrease in Zn^{2+} uptake (23%; $P < 0.01$) relative to the level for the wild type, with the Zn^{2+} acquisition entirely dependent on AdcAII. The up-

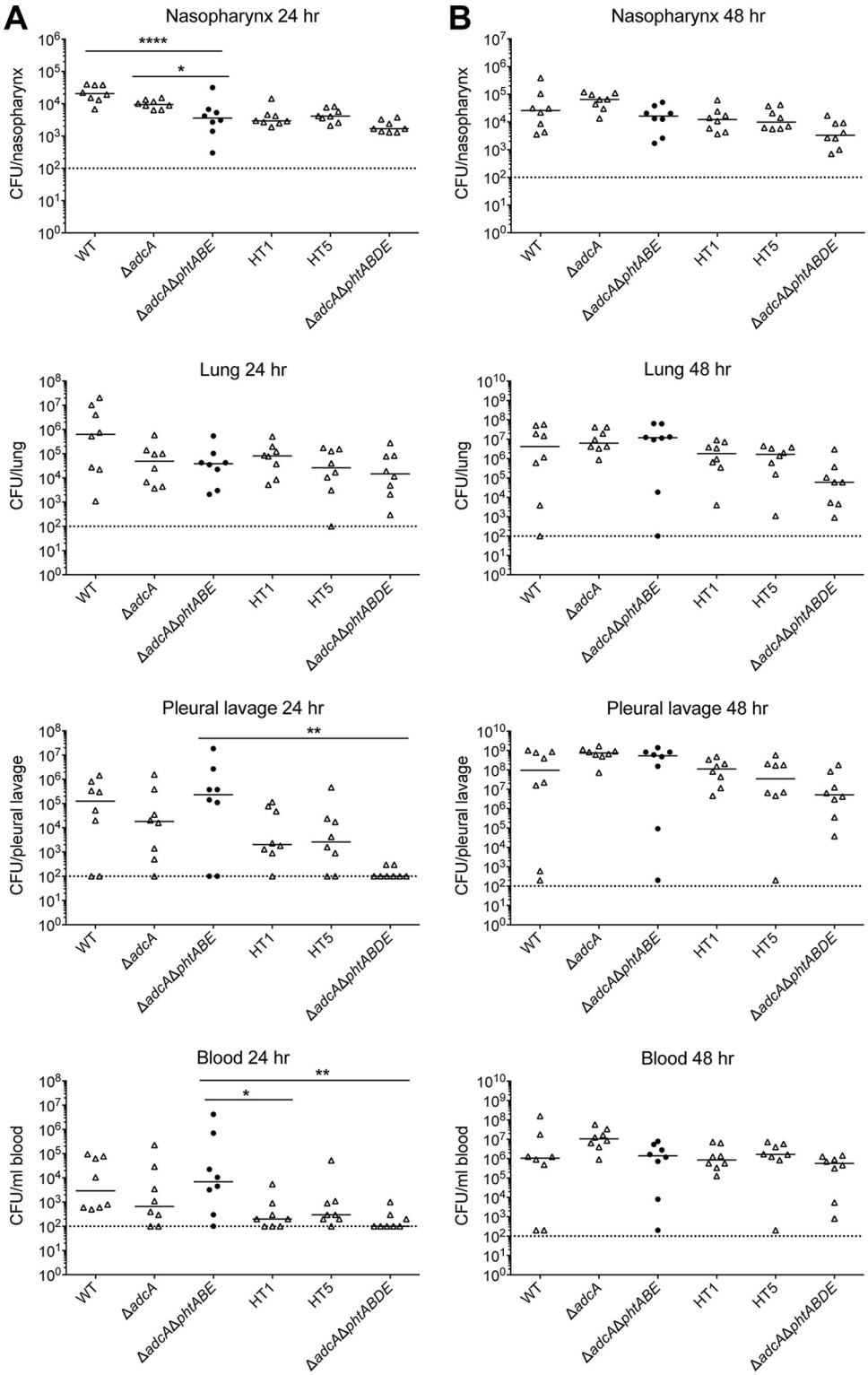

FIG 5 Burden of *S. pneumoniae* infection was assessed by determination of the bacterial load (CFU ml^{-1}) recovered from infected mice at 24 h (A) and 48 h (B) after challenge. The number of pneumococci in each niche at each time point is plotted (one point represents one niche from one mouse). Solid lines denote the median of each group; dashed lines denote the limit of detection. Statistically significant differences from the Δ*adcA* Δ*phtABE* mutant (circles) are indicated, as assessed by one-way ANOVA (*, $P < 0.05$; **, $P < 0.01$; ****, $P < 0.0001$).

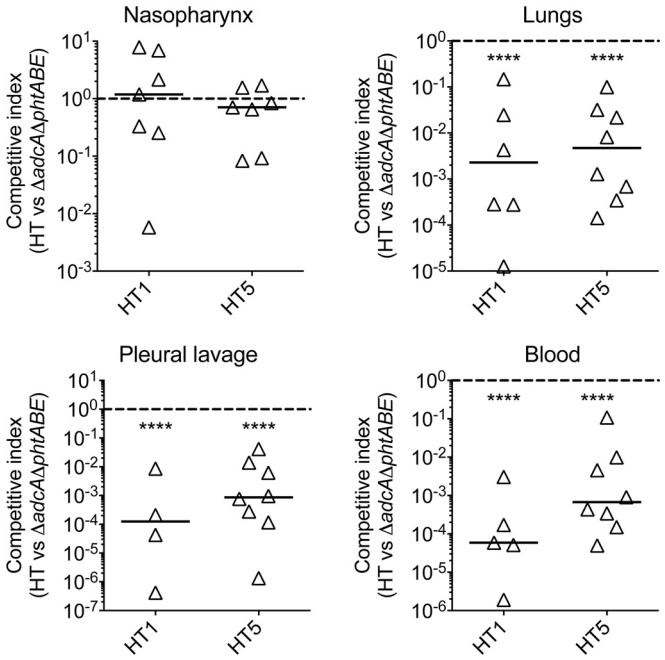

FIG 6 *In vivo* competition between the Δ*adcA* Δ*phtABE* mutant and HT1 or HT5. Eight mice were used per group. The results are shown as the median competitive indices (the ratio of the HT mutant to the Δ*adcA* Δ*phtABE* mutant corrected for the input ratio). The competitive index was compared to a theoretical mean of 1 (dashed line) by one-sample *t* tests, and the statistical significance is indicated (****, $P < 0.0001$).

take of Zn^{2+} was also significantly reduced in the HT1, HT2, HT3, and HT4 strains (~25%), but consistent with the expression and growth data, mutation of the HT5 site had no effect on Zn^{2+} accumulation. Overall, these data show that although total cellular Zn^{2+} accumulation was not found to be significantly different in any of the HT mutant strains, active Zn^{2+} uptake was impaired when any of the first four HT sites of PhtD were mutated. In contrast, the HT5 site, located at the carboxyl terminus of PhtD, appears to be the least important site for Zn^{2+} acquisition.

Role of PhtD HT sites *in vivo*. To examine whether the HT1 site also played a critical role during pneumococcal infection, we assessed the ability of the HT1 mutant strain to colonize and persist in various niches in a murine host. Colonization by the HT1 strain was compared to that of the *S. pneumoniae* D39 wild-type, Δ*adcA*, Δ*adcA* Δ*phtABE*, Δ*adcA* Δ*phtABDE* and HT5 mutant strains at 24 and 48 h. At 24 h the wild-type strain, and to a lesser degree the Δ*adcA* strain, was able to colonize various niches to a greater extent than the Δ*adcA* Δ*phtABE* strain, with a significantly higher level of colonization observed for the wild-type strain in the nasopharynx (Fig. 5A). To assess the impact of the HT mutations in PhtD, we first established the difference in colonization between the PhtD-only strain (Δ*adcA* Δ*phtABE*) and the strain lacking all Pht proteins (Δ*adcA* Δ*phtABDE*). Statistically significant differences (one-way ANOVA) between these two strains were only observed in the blood ($P < 0.01$) and pleural lavage fluid ($P < 0.01$) at 24 h postchallenge (Fig. 5A). Further analysis of these niches at 24 h revealed that results for the HT1 mutant strain were significantly different ($P < 0.05$) from results for the PhtD-only containing strain (Δ*adcA* Δ*phtABE*) in the blood but not in the pleural lavage fluid. Although not statistically significant, colonization of the HT5 mutant was also attenuated relative to that of the PhtD-only containing strain, and no statistically significant difference was observed between the HT1 and HT5 mutant strains. The lungs and pleural lavage fluid of the majority of mice infected with the HT1 or HT5 strain showed levels of bacterial burden intermediate between the parental strain (Δ*adcA* Δ*phtABE*) and the complete *pht* deletion strain (Δ*adcA* Δ*phtABDE*). As a consequence, the absolute quantitation of bacterial colonization did not allow for discrimination of the *in vivo* fitness between the HT mutants. To examine their colonization potential in greater detail, we then conducted an *in vivo* competition assay, in which mice were challenged with the HT1 or HT5 mutant strain and an equal dose of the parent strain (Δ*adcA* Δ*phtABE*). Since a number of mice infected with the HT mutant strains did not show detectable levels of bacteria in the blood 24 h postchallenge (Fig. 5A), we only examined the competitive index at 48 h. Both the HT1 and HT5 mutant strains were significantly compromised in their ability to infect the lungs, pleural cavity, and blood compared to the Δ*adcA* Δ*phtABE* strain (one-sample *t* test; $P < 0.0001$) (Fig. 6). The low competitive index of the HT5 mutant strain, relative to that of the Δ*adcA* Δ*phtABE* strain, was unanticipated given the *in vitro* characteristics of the strain, wherein the HT5 mutant was essentially comparable to the Δ*adcA* Δ*phtABE* strain in terms of Zn^{2+} uptake. Altogether, despite the differences between the HT mutants and the parent strain, no significant differences were seen in the competitive indices between the individual HT mutants. The observation that this finding does not directly correlate with the *in vitro* data suggests that the role of the individual HT motifs is more complex than first anticipated and worthy of further investigation.

DISCUSSION

Zinc acquisition in the pneumococcus is central to its ability to colonize and cause disease. As surface-associated proteins, the Pht family are proposed to hold key roles in aiding delivery of Zn^{2+} to AdcAII for transport by AdcCB under Zn^{2+}-limiting conditions, although the molecular details of the Zn^{2+} transfer process remain unclear. As the most highly conserved Pht protein, PhtD has been extensively studied and holds potential as a novel protein-based vaccine candidate. However, the roles of the individual HT motifs have not been thoroughly investigated. Here we have shown that, *in vitro*, the HT1 site is most important for growth in Zn^{2+}-restricted media, where the phenotypic impact was similar to that observed for a mutant lacking all Pht proteins. Overall, our *in vitro* data indicate a hierarchy of importance, where the HT site(s) at the amino terminus, i.e., closest to the cell membrane, has the most significant role in Zn^{2+} acquisition, whereas the HT5 site at the carboxyl terminus, which is closest to the extracellular environment, has the smallest contribution. Similar to other cluster A-I SBPs, AdcAII is anticipated to have an affinity for Zn^{2+} of $<$20 nM, facilitating this transfer and the delivery of Zn^{2+} to the AdcCB transporter. Notably, the amino termini of the different Pht proteins are also the most highly conserved portion of the protein, but the significance of this remains to be determined.

Intriguingly, while the hierarchy of importance of the HT sites holds true *in vitro*, the situation *in vivo* appears to be more complex. Although the HT1 site played a greater role in Zn^{2+} acquisition *in vitro*, the HT1 and HT5 strains were each similarly less competitive than the Δ*adcA* Δ*phtABE* strain, in a murine model of disease. A role for Pht proteins other than in AdcAII-mediated zinc recruitment was also demonstrated by an Δ*adcAII* Δ*phtABDE* deletion mutant, which was significantly impaired in its ability to cause invasive disease compared to an Δ*adcAII* strain (5). PhtD, together with the other Pht proteins, has previously been suggested to contribute to pneumococcal adherence to respiratory epithelial cells and aid in invasion (26) as well as contribute to the evasion of complement (27). Whether or not HT5, predicted to be the most surface-exposed HT motif, significantly contributes to any of these processes and thus disease progression requires further investigation. Alternatively, a functional HT5 motif may provide a competitive advantage for the acquisition of Zn^{2+} at the host-pathogen interface without significantly contributing to pneumococcal Zn^{2+} uptake.

In summary, the data presented here demonstrate that the PhtD HT sites hold an important role in Zn^{2+} acquisition and pneumococcal disease. Despite the significant advances made in uncovering the role of Pht proteins in pneumococcal Zn^{2+} acquisition, the precise pathway and molecular mechanism of Zn^{2+} movement across the capsule and cell wall barrier via the Pht proteins to AdcAII anchored to the outer face of the membrane require further analysis. Questions still remain as to the role of each of the HT sites in the translocation of Zn^{2+} and whether the Zn^{2+} is passed to AdcAII directly or indirectly from the Pht proteins. Further characterization of the overall role of the carboxyl-terminal HT sites *in vivo* will also be required to elucidate the manner in which they contribute to disease pathogenesis.

ACKNOWLEDGMENT

J.C.P. is an NHMRC Senior Principal Research Fellow.

FUNDING INFORMATION

Department of Industry, Innovation, Science, Research and Tertiary Education, Australian Government | Australian Research Council (ARC) provided funding to James C Paton under grant number DP120101432. Department of Industry, Innovation, Science, Research and Tertiary Education, Australian Government | Australian Research Council (ARC) provided funding to James C Paton and Christopher McDevitt under grant numbers DP120103957 and DP150101856. Department of Health | National Health and Medical Research Council (NHMRC) provided funding to James C Paton under grant numbers 565526 and 1071659. Department of Health | National Health and Medical Research Council (NHMRC) provided funding to Christopher McDevitt under grant numbers 1022240 and 1080784.

The funders had no role in study design, data collection and interpretation, or the decision to submit the work for publication.

REFERENCES

1. **Walker CL, Rudan I, Liu L, Nair H, Theodoratou E, Bhutta ZA, O'Brien KL, Campbell H, Black RE.** 2013. Global burden of childhood pneumonia and diarrhoea. Lancet **381:**1405–1416. http://dx.doi.org/10.1016/S0140-6736(13)60222-6.
2. **Bayle L, Chimalapati S, Schoehn G, Brown J, Vernet T, Durmort C.** 2011. Zinc uptake by *Streptococcus pneumoniae* depends on both AdcA and AdcAII and is essential for normal bacterial morphology and virulence. Mol Microbiol **82:**904–916. http://dx.doi.org/10.1111/j.1365-2958.2011.07862.x.
3. **Lewis VG, Ween MP, McDevitt CA.** 2012. The role of ATP-binding cassette transporters in bacterial pathogenicity. Protoplasma **249:**919–942. http://dx.doi.org/10.1007/s00709-011-0360-8.
4. **Plumptre CD, Eijkelkamp BA, Morey JR, Behr F, Counago RM, Ogunniyi AD, Kobe B, O'Mara ML, Paton JC, McDevitt CA.** 2014. AdcA and AdcAII employ distinct zinc acquisition mechanisms and contribute additively to zinc homeostasis in *Streptococcus pneumoniae*. Mol Microbiol **91:**834–851. http://dx.doi.org/10.1111/mmi.12504.
5. **Plumptre CD, Hughes CE, Harvey RM, Eijkelkamp BA, McDevitt CA, Paton JC.** 2014. Overlapping functionality of the Pht proteins in zinc homeostasis of *Streptococcus pneumoniae*. Infect Immun **82:**4315–4324. http://dx.doi.org/10.1128/IAI.02155-14.
6. **Plumptre CD, Ogunniyi AD, Paton JC.** 2012. Polyhistidine triad proteins of pathogenic streptococci. Trends Microbiol **20:**485–493. http://dx.doi.org/10.1016/j.tim.2012.06.004.
7. **Plumptre CD, Ogunniyi AD, Paton JC.** 2013. Surface association of Pht proteins of *Streptococcus pneumoniae*. Infect Immun **81:**3644–3651. http://dx.doi.org/10.1128/IAI.00562-13.
8. **Loisel E, Chimalapati S, Bougault C, Imberty A, Gallet B, Di Guilmi AM, Brown J, Vernet T, Durmort C.** 2011. Biochemical characterization of the histidine triad protein PhtD as a cell surface zinc-binding protein of pneumococcus. Biochemistry **50:**3551–3558. http://dx.doi.org/10.1021/bi200012f.
9. **Godfroid F, Hermand P, Verlant V, Denoel P, Poolman JT.** 2011. Preclinical evaluation of the Pht proteins as potential cross-protective pneumococcal vaccine antigens. Infect Immun **79:**238–245. http://dx.doi.org/10.1128/IAI.00378-10.
10. **Prymula R, Pazdiora P, Traskine M, Ruggeberg JU, Borys D.** 2014. Safety and immunogenicity of an investigational vaccine containing two common pneumococcal proteins in toddlers: a phase II randomized clinical trial. Vaccine **32:**3025–3034. http://dx.doi.org/10.1016/j.vaccine.2014.03.066.
11. **Plumptre CD, Ogunniyi AD, Paton JC.** 2013. Vaccination against *Streptococcus pneumoniae* using truncated derivatives of polyhistidine triad protein D. PLoS One **8:**e78916. http://dx.doi.org/10.1371/journal.pone.0078916.
12. **Ferreira DM, Jambo KC, Gordon SB.** 2011. Experimental human pneumococcal carriage models for vaccine research. Trends Microbiol **19:**464–470. http://dx.doi.org/10.1016/j.tim.2011.06.003.
13. **Pauksens K, Nilsson AC, Caubet M, Pascal TG, Van Belle P, Poolman**

JT, Vandepapeliere PG, Verlant V, Vink PE. 2014. Randomized controlled study of the safety and immunogenicity of pneumococcal vaccine formulations containing PhtD and detoxified pneumolysin with alum or adjuvant system AS02V in elderly adults. Clin Vaccine Immunol **21:**651–660. http://dx.doi.org/10.1128/CVI.00807-13.

14. **Rioux S, Neyt C, Di Paolo E, Turpin L, Charland N, Labbe S, Mortier MC, Mitchell TJ, Feron C, Martin D, Poolman JT.** 2011. Transcriptional regulation, occurrence and putative role of the Pht family of *Streptococcus pneumoniae*. Microbiology **157:**336–348. http://dx.doi.org/10.1099/mic.0.042184-0.
15. **Bersch B, Bougault C, Roux L, Favier A, Vernet T, Durmort C.** 2013. New insights into histidine triad proteins: solution structure of a *Streptococcus pneumoniae* PhtD domain and zinc transfer to AdcAII. PLoS One **8:**e81168. http://dx.doi.org/10.1371/journal.pone.0081168.
16. **Ilari A, Alaleona F, Tria G, Petrarca P, Battistoni A, Zamparelli C, Verzili D, Falconi M, Chiancone E.** 2014. The *Salmonella enterica* ZinT structure, zinc affinity and interaction with the high-affinity uptake protein ZnuA provide insight into the management of periplasmic zinc. Biochim Biophys Acta **1840:**535–544. http://dx.doi.org/10.1016/j.bbagen.2013.10.010.
17. **Riboldi-Tunnicliffe A, Isaacs NW, Mitchell TJ.** 2005. 1.2 Angstroms crystal structure of the *S. pneumoniae* PhtA histidine triad domain a novel zinc binding fold. FEBS Lett **579:**5353–5360. http://dx.doi.org/10.1016/j.febslet.2005.08.066.
18. **Ogunniyi AD, Grabowicz M, Mahdi LK, Cook J, Gordon DL, Sadlon TA, Paton JC.** 2009. Pneumococcal histidine triad proteins are regulated by the Zn^{2+}-dependent repressor AdcR and inhibit complement deposition through the recruitment of complement factor H. FASEB J **23:**731–738. http://dx.doi.org/10.1096/fj.08-119537.
19. **McDevitt CA, Ogunniyi AD, Valkov E, Lawrence MC, Kobe B, McEwan AG, Paton JC.** 2011. A molecular mechanism for bacterial susceptibility to zinc. PLoS Pathog **7:**e1002357. http://dx.doi.org/10.1371/journal.ppat.1002357.
20. **Begg SL, Eijkelkamp BA, Luo Z, Counago RM, Morey JR, Maher MJ, Ong CL, McEwan AG, Kobe B, O'Mara ML, Paton JC, McDevitt CA.** 2015. Dysregulation of transition metal ion homeostasis is the molecular basis for cadmium toxicity in *Streptococcus pneumoniae*. Nat Commun **6:**6418. http://dx.doi.org/10.1038/ncomms7418.
21. **Eijkelkamp BA, Morey JR, Ween MP, Ong CL, McEwan AG, Paton JC, McDevitt CA.** 2014. Extracellular zinc competitively inhibits manganese uptake and compromises oxidative stress management in *Streptococcus pneumoniae*. PLoS One **9:**e89427. http://dx.doi.org/10.1371/journal.pone.0089427.
22. **Clementi EA, Marks LR, Roche-Hakansson H, Hakansson AP.** 2014. Monitoring changes in membrane polarity, membrane integrity, and intracellular ion concentrations in *Streptococcus pneumoniae* using fluorescent dyes. J Vis Exp **2014:**e51008. http://dx.doi.org/10.3791/51008.
23. **Adamou JE, Heinrichs JH, Erwin AL, Walsh W, Gayle T, Dormitzer M, Dagan R, Brewah YA, Barren P, Lathigra R, Langermann S, Koenig S, Johnson S.** 2001. Identification and characterization of a novel family of pneumococcal proteins that are protective against sepsis. Infect Immun **69:**949–958. http://dx.doi.org/10.1128/IAI.69.2.949-958.2001.
24. **Beghetto E, Gargano N, Ricci S, Garufi G, Peppoloni S, Montagnani F, Oggioni M, Pozzi G, Felici F.** 2006. Discovery of novel *Streptococcus pneumoniae* antigens by screening a whole-genome lambda-display library. FEMS Microbiol Lett **262:**14–21. http://dx.doi.org/10.1111/j.1574-6968.2006.00360.x.
25. **Shafeeq S, Kloosterman TG, Kuipers OP.** 2011. Transcriptional response of *Streptococcus pneumoniae* to Zn^{2+} limitation and the repressor/activator function of AdcR. Metallomics **3:**609–618. http://dx.doi.org/10.1039/c1mt00030f.
26. **Kallio A, Sepponen K, Hermand P, Denoel P, Godfroid F, Melin M.** 2014. Role of Pht proteins in attachment of *Streptococcus pneumoniae* to respiratory epithelial cells. Infect Immun **82:**1683–1691. http://dx.doi.org/10.1128/IAI.00699-13.
27. **Melin M, Di Paolo E, Tikkanen L, Jarva H, Neyt C, Kayhty H, Meri S, Poolman J, Vakevainen M.** 2010. Interaction of pneumococcal histidine triad proteins with human complement. Infect Immun **78:**2089–2098. http://dx.doi.org/10.1128/IAI.00811-09.